

# Parameterization of two-dimensional turbulence using an anisotropic maximum entropy production principle

F. BOUCHET<sup>1,2</sup>

<sup>1</sup>Institut Fourier, UMR 5582, Grenoble France

<sup>2</sup>Dipartimento di Energetica “Sergio Stecco”, Università degli studi di Firenze, Italy

22nd December 2018

Received:

Author version:

Author contact : bouchet@dma.unifi.it

## Abstract

We consider the modeling of the effect of unresolved scales, for two-dimensional and geophysical flows. We first show that the effect of small scales on a coarse-grained field, can be approximated at leading order, by the effect of the strain tensor on the gradient of the vorticity, which exactly conserves the energy. We show that this approximation would lead to unstable numerical code. In order to propose a stable parameterization, while taking into account of these dynamical properties, we apply a maximum entropy production principle. The parameterization acts as a selective diffusion proportional to the mean strain, in the contraction direction, while conserving the energy. We show on numerical computation that the obtained anisotropic relaxation equations give an important predictability improvement, with respect to Navier-Stokes, Smagorinsky or hyperviscous parameterizations.

# 1 Introduction

Turbulent flows are characterized by the non-linear interaction of a huge number of variables. For very high Reynolds' numbers, the current or foreseen computational capabilities only permit to describe part of corresponding degrees of freedom. For instance, for geophysical flows, the molecular viscosity acts at typical scales of order of the millimeter, whereas a current typical resolution for meteorological computations is about 30 to 50 *km*. The issue of the parameterization of the effect of unresolved scale on the actually described ones is thus of crucial importance.

The predominance of the Coriolis force and the density stratification give geophysical flows a quasi two-dimensional nature. Their organization is actually three dimensional, but may be well approximate by layered models [1]. Moreover, at large scale, an inverse energy-cascade process (from small to large scale), typical of two-dimensional flows, is observed for geophysical flows. In the following, we address the issue of small scale turbulence parameterization in both the frameworks of the two-dimensional incompressible Euler equation, or of the Quasi-Geostrophic model on the other hand.

Any numerical resolution of the flow dynamics implicitly assumes that an averaged value is described. The average of the nonlinear terms should then be expressed in terms of the known averages of the single quantities. This is the classical closure problem for flow equations [2]. In order to clearly specify the problem, one has to precise the meaning of the average. When a statistically stationary situation is identified, a very natural choice is an ensemble average on the stationary distribution. For instance, this would be the case, for an inverse cascade regime (a small scale energy injection and a large scale drag force) where a natural ensemble is given by a stationary probability distribution for this process. The proximity of such a stationary situation is implicitly assumed, together with other hypothesis, in classical parameterizations such as the Eddy Damped Quasi Markovian Model (EDQNM) [3, 4, 5] or the  $K - \epsilon$  model [4]. An other approach is to specify the stochastic properties of the unresolved scales, as for instance in the Direct Interaction Approximation (DIA) [7].

However, geophysical flows are characterized by the existence of large scales structures (jets, cyclone and anticyclones), which break the self-similarity at the base of the description of the inverse cascade process. The typical time scales for forcing and dissipation are much larger than the inertial ones. In order to study such flows, we will consider two dimensional inviscid models in a freely decaying-turbulence regime. In such a case, for large times, the flow self-organize in coherent structures. The final state may be described by the statistical mechanics of the vorticity (or the potential vorticity) [9, 10]. For such a freely decaying turbulence, and in a situation close to the equilibrium or to a quasi-stationary state of the inviscid equations, it would be very natural to consider an ensemble average, compatible with the observed large scale structure and vorticity distribution. Such an ensemble average is for instance implicitly assume in the kinetic approach of Chavanis [11]. On the contrary, in this work, we will be interested in situations far from equilibrium or

from stationary solutions (vortex merging, filamentation). In such a case, there is no natural statistical ensemble to consider. Moreover, we will show that for a given flow evolution, the effect of unresolved scales will be dominated by structures (filaments) which are strongly correlated with the resolved scales. Given this situation, we will consider the evolution of locally averaged quantities, on the grid scale  $l$  (average by homogenization by opposition of ensemble average).

In section 2 we recall the equation of motion and give the formal properties of an average by homogenization. We then show that the averaged equations will be determined by the knowledge of a turbulent current. In section 3, we give an analytic expression of this turbulent current, at leading order in an asymptotic expansion in power of the ratio of grid scale on the domain scale  $l/L$ . The turbulent current is then expressed in terms of the averaged velocity strain tensor. This result has been described in [14] and independently in [16, 15]. We discuss the validity of this deterministic approximation. Using numerical integration, we show that this expression is actually a very good approximation of the actual turbulent current, in situations of decaying turbulence, far from equilibrium. This deterministic approximation exactly conserves the energy of the mean flow.

As the strain tensor is of zero trace, its two eigenvalues are opposite. They respectively correspond to a positive and negative viscosity. For this reason, this deterministic approximation is not suited to model the effect of small scales in a numerical code: it would lead to instability of the scheme. In section 4, we obtain a stable algorithm by determining the turbulent current which maximize the production of the mixing entropy, while respecting both the value of the deterministic current in the stable direction of the strain tensor, and the conservation of energy. Such a maximum entropy production principle has already been used by Robert and Sommeria [12], but without taking into account for the anisotropy of the turbulent current. With this new specification, the obtained equations respect all the usable properties of the deterministic current, and have the further property to converge towards equilibrium of the statistical mechanics. In section 5, we compare the performance of these *anisotropic relaxation equations* with other models, commonly used to parameterize small scale turbulence, for two-dimensional or geophysical flows: the eddy viscosity model, the Smagorinsky model [13], and an hyperviscosity parameterization. In section 5, the anisotropic relaxation equation are shown to give the best results, when compared with high resolution simulation, both for the Euler and for the Quasi-Geostrophic equations.

In section 6, we discuss these results and their interest for geophysical flow applications.

## 2 The averaged equations of motion

In this section, we recall the two-dimensional incompressible Euler equations and the Quasi-Geostrophic model. We specify the average operator for the resolved dynamics and we give the main properties of the averaged equations of motion.

The incompressible Euler equations describe the evolution of the velocity  $\mathbf{u}$  of an incompressible inviscid fluid. For 2D flows, they are equivalent to the equation for the evolution of the vorticity ( $\omega = (\nabla \wedge \mathbf{u}) \cdot \mathbf{e}_z$ ):

$$\frac{\partial \omega}{\partial t} + \mathbf{u} \cdot \nabla \omega = 0 \quad (1)$$

$$\omega = -\Delta \psi \quad (2)$$

$$\mathbf{u} = -\mathbf{e}_z \wedge \nabla \psi \quad (3)$$

The vorticity  $\omega$  is advected by the divergence-less velocity  $\mathbf{u}$ ,  $\psi$  is the stream-function. For sake of simplicity, we will consider these equation on a torus  $D$  (all the quantities are periodic in both variables, with zero global average). All our discussion is easily generalizable for any bounded domain  $D$  (an impermeability condition  $\mathbf{u} \cdot \mathbf{n}$ , where  $\mathbf{n}$  is normal to the boundary of  $D$  would then specify the boundary conditions).

The Euler equations conserve the energy :

$$E = \frac{1}{2} \int_D d\mathbf{r} \mathbf{u}^2 = \frac{1}{2} \int_D d\mathbf{r} \omega \psi \quad (4)$$

and all the functionals of the form  $C_f(\omega) = \int_D d\mathbf{r} f(\omega)$  for any function  $f$ . The Quasi-Geostrophic (QG) equation, which is the simplest model of geophysical flows [1], are :

$$\frac{\partial q}{\partial t} + \mathbf{u} \cdot \nabla q = 0 \quad (5)$$

$$q = -\Delta \psi + \frac{\psi}{R^2} \quad (6)$$

We note the formal similarity with the Euler equation. The potential vorticity  $q$  is then advected. The determination of the stream function, is then given by the inversion of the equation (6), and the velocity is still given by (3). The energy for the QG dynamics is  $E = 1/2 \int_D d\mathbf{r} [\mathbf{u}^2 + \psi^2/R^2] = 1/2 \int_D d\mathbf{r} q\psi$ . One clearly see the strong analogies between the QG and the Euler equations. From now on, we will deal only with the Euler equation. We will precise when the generalization for the QG equation is not straightforward.

Our aim is to obtain the equation describing the evolution of the spatial average of the velocity and of the vorticity. We define the average  $\overline{f}$  of any quantity  $f$  by :

$$\overline{f(\mathbf{r})} = \int_D d\mathbf{r}' G^l(\mathbf{r} - \mathbf{r}') f(\mathbf{r}')$$

This operator is the convolution with  $G$ . We suppose that  $\int d\mathbf{r} G(\mathbf{r}) = 1$  and that  $G$  is invariant under any rotation ( $G(\mathbf{r})$  only depends on the modulus of  $\mathbf{r}$ .) The qualitative properties assumed for  $G$  are to regularize the field at a fixed scale  $l$ . For instance, in section 3, we will use in the  $2\pi$ -periodic domain the kernel  $G^l$  whose Fourier components

are  $G_{\mathbf{k}}^l = \frac{1}{(2\pi)^2} \exp\left(-\frac{l^2 k^2}{2}\right)$ ,  $\mathbf{k} \in \mathbf{Z}^2$  (when  $l$  is much smaller than  $2\pi$ ,  $G^l(\mathbf{r})$  is close to  $\frac{1}{2\pi l^2} \exp\left(-\frac{r^2}{2l^2}\right)$ ). The average operator verifies the linearity property :  $\overline{f + \lambda g} = \overline{f} + \lambda \overline{g}$  and the commutation with the differential operators :  $\partial_i \overline{f} = \overline{\partial_i f}$ . We note that it does not verify the properties  $\overline{\overline{f}} = \overline{f}$  and  $\overline{f\overline{g}} = \overline{f}\overline{g}$  as would be the case for an ensemble average. In section 3, we will show that the dominant contribution of the turbulent current comes from the non-verification of these two properties.

By averaging (1), we obtain the averaged Euler equation :

$$\frac{\partial \overline{\omega}}{\partial t} + \overline{\mathbf{u}} \cdot \nabla \overline{\omega} = -\nabla \cdot \mathbf{J}_\omega \quad \text{with } \mathbf{J}_\omega = \overline{\omega \mathbf{u}} - \overline{\omega} \overline{\mathbf{u}} \quad (7)$$

$$\overline{\omega} = -\Delta \overline{\psi} \quad (8)$$

$$\overline{\mathbf{u}} = -\mathbf{e}_z \wedge \nabla \overline{\psi} \quad (9)$$

We note that the correlation term is the divergence of a current  $\mathbf{J}_\omega$ , that we will call the turbulent current. We note that the average Euler equations have the same symmetry property than the initial Euler equations.

The aim of our study is to determine an expression of the turbulent current  $\mathbf{J}_\omega$  in terms of the average quantities. This closure problem is equivalent to the usual one for the velocity correlations, when the evolution of the velocity is considered.

### 3 Anisotropy of the turbulent current

In this section, we first derive an approximation of the turbulent current, as the leading order of an expansion in power of the homogenization scale  $l$  (the actual expansion parameter is  $l/L$ , where  $L$  is a typical size of the domain  $D$ ). We discuss the main properties of this deterministic expression. The turbulent current is anisotropic. It is related to the symmetric part of the strain tensor for the averaged velocity. It exactly conserves the energy of the averaged fields. Using typical vorticity fields of freely decaying turbulence, we numerically compute the actual turbulent current, in order to study the validity of this first order approximation.

#### 3.1 A leading order deterministic approximation

In order to obtain an approximation of the turbulent current  $\mathbf{J}_\omega$ , we decompose the vorticity field as the sum of its average  $\overline{\omega}$  and of fluctuations  $\tilde{\omega}$ ,  $\tilde{\omega}$  being defined by  $\omega = \overline{\omega} + \tilde{\omega}$ . Similarly  $\mathbf{u} = \overline{\mathbf{u}} + \tilde{\mathbf{u}}$ . We then obtain for the turbulent current  $\mathbf{J}_\omega$  (7) :

$$\mathbf{J}_\omega \equiv \overline{\omega \mathbf{u}} - \overline{\omega} \overline{\mathbf{u}} = \underbrace{(\overline{\omega \mathbf{u}} - \overline{\omega} \overline{\mathbf{u}})}_{\mathbf{J}_d} + \underbrace{\overline{\tilde{\omega} \mathbf{u}} + \overline{\omega \tilde{\mathbf{u}}}}_{\mathbf{J}_s} \quad (10)$$

We note that the first term (double average), the second term (correlation between the vorticity fluctuations and the mean velocity) and the third term (correlation between the velocity fluctuations and the mean velocity) are all identically equal to zero for an ensemble average. The decomposition (10) is the commonly used one. However, for reason that shall become clear we will use :

$$\mathbf{J}_\omega = \mathbf{J}_d + \mathbf{J}_s \quad \text{with} \quad \mathbf{J}_d = \overline{\overline{\mathbf{u}}} + \overline{\tilde{\omega}\mathbf{u}} - \overline{\omega}\mathbf{u} \quad \text{et} \quad \mathbf{J}_s = \overline{\tilde{\omega}\tilde{\mathbf{u}}} + \overline{\tilde{\omega}\mathbf{u}} \quad (11)$$

The first term  $\mathbf{J}_d$ , which does not depend on the velocity fluctuations, will be called the deterministic component of the turbulent current (we will show that it can be expressed, to a good approximation, in terms of the averaged quantities). The second term depends on the velocity fluctuations. It will be called the stochastic component of the turbulent current. As the order of magnitude of  $\tilde{\mathbf{u}}$  is  $l$  times the order of magnitude of  $\mathbf{u}$ , we anticipate that the stochastic current will be negligible at leading order in  $l$ .

In order to relate the deterministic part of the turbulent current  $\mathbf{J}_d = \overline{\overline{\mathbf{u}}} - \overline{\omega}\mathbf{u}$  (11) to the strain tensor for the averaged velocity, we expand  $\mathbf{u}$  in Taylor series around a point  $O$ . By noting that the zeroth order terms are null, we obtain at the leading order in  $l$  :  $\mathbf{J}_d(O) = \overline{\overline{x}}(O) \partial_x \overline{u_x}(O) + \overline{\overline{y}}(O) \partial_y \overline{u_x}(O)$ . Using that the the average operator is equivalent to a Gaussian for small  $l$ , we note that a part-integration leads to  $\overline{\overline{x}}(O) = l^2 \partial_x \overline{\omega}(O)$  and  $\overline{\overline{y}}(O) = l^2 \partial_y \overline{\omega}(O)$ . Using this result, we obtain that the deterministic part of the turbulent current is equal, at leading order, to the action of the strain tensor on the vorticity gradient :

$$\mathbf{J}_d = l^2 \boldsymbol{\Sigma} \nabla \overline{\omega} \quad (\text{order } 1) \quad \text{with} \quad \boldsymbol{\Sigma} = \begin{pmatrix} \partial_x \overline{u_x} & \partial_y \overline{u_x} \\ \partial_x \overline{u_y} & \partial_y \overline{u_y} \end{pmatrix}$$

As the typical variation length for the mean vorticity  $\overline{\omega}$  is  $l$ , its gradient is of order  $1/l$ , and this expression is actually of order 1. This expansion may be led to any order in  $l$ . At each order it involves derivatives of  $\overline{\omega}$  at larger orders. In section 3.2 we will study numerically this approximation for vorticity fields typical of freely decaying turbulence, in the regime of vortex merging and filamentation.

The antisymmetric part of the strain tensor,  $\boldsymbol{\Sigma}_{ant}$ , characterizes the local rotation of the fluid. It is linked to the vorticity by :  $\boldsymbol{\Sigma}_{ant} = 2 \begin{pmatrix} 0 & \overline{\omega} \\ -\overline{\omega} & 0 \end{pmatrix}$ . It is easily verified that  $\nabla \cdot (\boldsymbol{\Sigma}_{ant} \nabla \overline{\omega}) = 0$ . Thus, whereas it is present in the leading order approximation for  $\mathbf{J}_d$ , this antisymmetric part has no effect on the evolution of the vorticity. We have :

$$\nabla \cdot \mathbf{J}_d = l^2 \nabla \cdot (\boldsymbol{\Sigma}_{sym} \nabla \overline{\omega}) \quad (\text{order } 1) \quad \text{with} \quad \boldsymbol{\Sigma}_{sym} = \begin{pmatrix} \partial_x \overline{u_x} & (\partial_y \overline{u_x} + \partial_x \overline{u_y}) / 2 \\ (\partial_y \overline{u_x} + \partial_x \overline{u_y}) / 2 & \partial_y \overline{u_y} \end{pmatrix} \quad (12)$$

The symmetric part of the strain tensor may be diagonalized with orthogonal eigenvectors. As the fluid is incompressible, it has a null trace and thus has two opposite eigenvalues  $\sigma$  et  $-\sigma$ , with eigenvectors  $\mathbf{e}_\sigma$  and  $\mathbf{e}_{-\sigma}$  respectively.  $\sigma$  is the mean strain :

$$\sigma = \sqrt{-\det(\boldsymbol{\Sigma}_{sym})} = \sqrt{-\partial_x u_x \partial_y u_y + (\partial_y u_x - \partial_x u_y)^2 / 4}$$

Let us consider the operator  $\bar{\omega} \rightarrow \int_D d\mathbf{r} \bar{\omega} \nabla \cdot (\boldsymbol{\Sigma}_{sym} \nabla \bar{\omega})$ . The contraction direction of the strain tensor  $\mathbf{e}_\sigma$  corresponds to the definite negative part of this operator : for any  $\bar{\omega}$ ,  $\int_D d\mathbf{r} \bar{\omega} \nabla \cdot (\mathbf{e}_\sigma \mathbf{e}_\sigma^T \nabla \bar{\omega}) < 0$  (by part integration). It thus acts as a positive viscosity. Conversely, the stretching direction of the strain  $\mathbf{e}_{-\sigma}$  tensor will correspond to the positive part of this operator. It thus act as a negative viscosity. We will note  $\boldsymbol{\Sigma}_{sym} = \boldsymbol{\Sigma}_{sym}^> + \boldsymbol{\Sigma}_{sym}^<$  with  $\boldsymbol{\Sigma}_{sym}^< = \sigma \mathbf{e}_\sigma \mathbf{e}_\sigma^T$  and  $\boldsymbol{\Sigma}_{sym}^> = -\sigma \mathbf{e}_{-\sigma} \mathbf{e}_{-\sigma}^T$  where  $T$  is the transposition. From a numerical point of view, the negative part of the symmetric part of the strain tensor  $\boldsymbol{\Sigma}_{sym}^<$  will have a stabilization effect whereas the positive part  $\boldsymbol{\Sigma}_{sym}^>$  will have a destabilization effect. In a numerical code, this last term will lead to instabilities. For this reason, the approximate expression (12) does not suit for a direct parameterization of the effect of small scales on large scales.

To conclude this analysis, we note that the leading order approximation of the turbulent current (12) exactly conserves the energy of the averaged field :  $\overline{E} = \frac{1}{2} \int_D d\mathbf{r} \bar{\mathbf{u}}^2 = \frac{1}{2} \int_D d\mathbf{r} \bar{\omega} \bar{\psi}$ . The conservation of the energy is a key property of two-dimensional turbulence. In section 3.2, we will show numerically that the actual turbulent current (not the leading order approximation) is responsible for a very small flux of energy towards the large scale ( $\overline{E}$  slightly increase). This is in accordance with the phenomenology of two-dimensional freely decaying turbulence.

We have described a leading order approximation for the turbulent current. This approximation is deterministic (it can be expressed explicitly in terms of the averaged quantities). The turbulent current is the application of the strain tensor on the gradient of the mean vorticity. This approximation exactly conserves the energy. In the following section we will show numerically that this approximation is a go one for typical vorticity fields. However, this analytical expression can not be used to design a stable numerical scheme. In section 4, we will propose a stable scheme that respects the main properties of this approximation.

### 3.2 Numerical analysis of the turbulent current

For a given vorticity field, it is possible to compute numerically the averaged field at a given scale. From it, one can then compute the turbulent current. The aim of this section is to describe qualitatively the turbulent current, and to study the validity of the leading order approximation, for vorticity fields which are typical of freely decaying turbulence.

In order to obtain freely decaying turbulence typical vorticity fields, we use results of numerical simulations. For all numerical computations of this article, we will use a pseudo-spectral code, with an order 3 Adam-Bradsforth scheme for the temporal discretisation, on

a domain periodic in both direction. The result are presented for a vorticity field obtained by numerically solving the Navier Stokes equations :

$$\frac{\partial \omega}{\partial t} + \mathbf{u} \cdot \nabla \omega = \nu \Delta \omega \quad (13)$$

For a given resolution, the viscosity  $\nu$  is chosen as small as possible, such that the computation is stable. The Navier Stokes equation verify a maximum principle : the maxima (resp. minima) of the vorticity must always decrease (resp. increase) in time. In order to test the stability of the computation, we check for any computation the extrema of the vorticity. We have studied the turbulent current for several situations. We discuss the results for the vorticity field represented on Fig. 1. It has been obtained by considering an initial condition made of random patches of potential vorticity. The typical vorticity and velocity are of order 1. The parameter of the computation are  $\nu = 3.14 \cdot 10^{-5}$ ,  $Re = 2\pi u_{max}/\nu = 200000$ ,  $dt = 6.14 \cdot 10^{-4}$  (time step), resolution  $1024 \times 1024$ . The vorticity field is the one corresponding to  $t = 15$ . At this time, the decrease of the total energy is of order 2%, such that the Navier-Stokes approximation may be considered a good approximation of the Euler equation. A more precise description of the computation is given in Bouchet (2001).

This vorticity field is characteristic of the regime of strong filamentation, due to the nonlinear interaction between the vortex. Fig. 1 shows that coherent vortices are present together with filament structures, at all scale of the field. We will compute the averaged vorticity field, using the averaging operator described in section 2, with  $l = 2\pi/128$ . This corresponds to an homogenization at a scale corresponding to a numerical resolution  $128 \times 128$ . The corresponding averaged vorticity field is represented on Fig. 1.

From the averaged vorticity field, we compute the turbulent current  $\mathbf{J}_\omega = \overline{\omega \mathbf{u}} - \overline{\omega} \overline{\mathbf{u}}$ . Fig. 2 shows the divergence  $\nabla \cdot \mathbf{J}_\omega$  of the turbulent current, associated to the vorticity field  $\omega$ . The comparison of this picture with the vorticity one (Fig. 1) clearly illustrates that the divergence of the turbulent current is associated to structures with typical scales of the order of the homogenization scale  $l$ . Most of these structures are filaments that are stretched by the flow strain, passing from resolved to unresolved scales. Fig. 3 shows the mean strain  $\sigma$ , for the averaged velocity field. The strain is a vectorial property. This figure however clearly show that areas with strong strain are associated with strong vorticity gradients (alignment of the structures with the strain), and that these areas are the ones that give strong contributions to the divergence of the turbulent current. This qualitative description is in accordance with the result we have obtained for the leading order approximation of the turbulent current by the effect of the strain tensor on the gradient of the vorticity field.

Let us analyze quantitatively the contribution of the various terms composing the turbulent current. Table 1 shows the divergence of the terms of the classical decomposition (10). This illustrates that the two first terms have a contribution much larger than the total turbulent current. We thus note that these two first current are strongly anti-correlated. Indeed their sum  $\mathbf{J}_d$  give a contribution much less important that each of its components.



Table 1 also shows that the principal contribution of  $\mathbf{J}_s$  is the correlation between vorticity fluctuations and velocity fluctuations. In a numerical simulation with resolved scales up to the scale  $l$ , this will correspond to the contribution of unresolved scales, for which any information is lost. A statistical modeling of this component will then be the more natural. That's why we call  $\mathbf{J}_s$ , the stochastic component of the turbulent current. The deterministic part dominates the stochastic part, by a factor 10 to 15, for the three studied norms. This is in accordance with the leading order approximation we have obtained in section 3.1.

Let us discuss the results obtained by Laval, Dubrulle and Nazarenko [17], for currents computed for an average corresponding to a spectral truncation of the vorticity field. They have studied the relative contribution of the currents 2, 3 et 4 (see 10). They have shown that the advection of the fluctuations by the average velocity (term 2) dominates the terms 3 and 4. This is in accordance with the result we have obtained with a Gaussian homogenization. Using these results, they have justified an approximation neglecting these last two terms. They have then proposed a parameterization of small scale effects, in which the second term is determined thanks to a particle description of the fluctuations [18]. We will follow another approach : we use a deterministic approximation of the sum of the two terms  $1+2=\mathbf{J}_d$ .

Table 2 shows the norms of the difference between  $\mathbf{J}_d$  and its first (12) and second order approximation, in the small  $l/L$  expansion. We conclude that, for this vorticity field, in the regime of vortex merging and strong filamentation, the deterministic part of the turbulent current can be approximated by the action of the strain tensor on the gradient of the vorticity, up to an error of order of 10%. Table 2 also shows the relative contribution of the positive and of the negative parts of the strain tensor. The negative part ( $\Sigma_{sym}^<$ , positive eigenvalue) has a larger contribution than the positive ones ( $\Sigma_{sym}^>$ , negative eigenvalue). This illustrates the irreversibility of the flow evolution : due to this property, the moments of the vorticity will evolve towards values corresponding to the further mixing of the vorticity. We however recall that energy loss associated to the negative part is exactly compensated by energy gain associated to the positive part.

## 4 Anisotropic relaxation equations

In section 3 we have obtained a deterministic approximation for the turbulent current  $\mathbf{J}_\omega$ . This approximation is the action of the strain tensor on the gradient of the vorticity. It exactly conserves the energy. However the positive part of the strain tensor acts similarly to a negative viscosity. This would render any numerical simulation unstable. In this section, in order to obtain a parameterization as close as possible to the actual turbulent current, but with the essential practical constraint to lead to a stable numerical scheme, we will search for a turbulent current which have the property of the deterministic one in the contraction direction of the strain tensor (stabilization effect), and which exactly conserves the energy.

There are several ways to impose such constraints to a parameterization. We choose

to determine a parameterization which is in accordance with the statistical properties of the mixing of the vorticity. Equilibrium statistical mechanics of the two-dimensional Euler equations describes the most probable mixing of the vorticity for a given distribution of potential vorticity and Energy. We will then choose the turbulent current which maximize the entropy production, while respecting the energy conservation and the effect of the stable contribution of the strain tensor.

A similar maximum entropy production principle (MEPP) has been used by Robert and Sommeria [12] in order to parameterize the small scale turbulence. In this work, author however impose an isotropic constraint on the turbulent current. We make a derivation very close to their one, but we impose the value of the turbulent current in the stable direction of the strain tensor. We thus explicitly take into account the anisotropic nature of the turbulent current. We do not think that such a maximum entropy production principle is based on any physical or theoretical ground. The anisotropic relaxation turbulent current will indeed be different from the observed one. We however use this principle to obtain stable equation as close as possible from the correct physical ones.

In section 5, we will show that the obtained anisotropic relaxation equations lead to better results than classical parameterizations in order to determine the evolution of coarse\_grained flow.

Let us first briefly introduce the results of the equilibrium statistical mechanics of the vorticity. In order to simplify this discussion, we will consider an initial condition made of many vorticity patches, but with only two values  $\omega = a_1$  and  $\omega = a_2$ , occupying respectively areas  $A_1$  and  $A_2$ . Generalization of this discussion and of the following results to any initial distribution of vorticity is however straightforward. We note that the initial distribution (values  $a_1$  and  $a_2$ , and areas  $A_1$  and  $A_2$ ) are conserved by the inviscid dynamics. We now consider a coarse-graining of the vorticity at a scale  $l$  (local-average at the scale  $l$ , which will be interpreted in our case, as the numerical resolution scale). At this coarse-grained scale (macroscopic description), we will describe the vorticity fields by the local probabilities  $p(\mathbf{r})$  and  $(1 - p(\mathbf{r}))$  to have respectively the vorticity values  $a_1$  and  $a_2$ , at the position  $\mathbf{r}$ . The expression of the coarse-grained vorticity is then :  $\bar{\omega} = a_1 p + a_2(1 - p)$ . The main result of the equilibrium statistical mechanics, is the evaluation of the probability to observe a local probability field  $p(\mathbf{r})$ , given the vorticity distribution a given energy  $E$ . When the scale  $l$  goes to zero, the logarithm of the probability of two probability fields is given by the entropy  $S$  :

$$S = \int_D d\mathbf{r} s(p) \quad \text{with} \quad s(p) = -(p \log p + (1 - p) \log(1 - p)) \quad (14)$$

(see [10, 9], and [20, 21] for a justification). The most probable state is then given by the maximization of the entropy for a given energy and vorticity distribution. This equilibrium is a stationary state of the dynamical equations. The main hypothesis of the equilibrium statistical mechanics is that the complex dynamical evolution of the flow will lead to a state

close to the equilibrium one.

We would like to describe the coarse grained evolution of the vorticity. On the contrary to the equilibrium case, no clear principle permits to describe this out of equilibrium relaxation. The Euler equations advect the two levels of vorticity with the velocity  $\mathbf{u}$ . This conservation equation will lead to a transport equation for  $p$ , by the mean velocity  $\bar{\mathbf{u}}$  on one hand, and by a turbulent current  $\mathcal{J}$  as a consequence of the unresolved scales :

$$\partial_t p + \bar{\mathbf{u}} \cdot \nabla p = -\nabla \cdot \mathcal{J} \quad (15)$$

Using the link between the averaged vorticity and the probability :  $\bar{\omega} = a_1 p + a_2(1 - p)$ , the coarse-grained vorticity verify equation (7) with  $\mathbf{J}_\omega = (a_1 - a_2)\mathcal{J}$ . Our aim is thus to determine  $\mathbf{J}_\omega$ .

As explained in the introduction, we look for a turbulent current which has a determined behavior in a direction given by the strain tensor and which conserve the energy. As this does not specify the turbulent current, in order to obtain an equation compatible with the statistical tendency of the equation to increase the entropy, we will look at equation which maximize the entropy production rate, given these dynamical constraints.

Using (15), we first compute the entropy and energy production rates :

$$\frac{dS}{dt} = - \int_D d\mathbf{r} \frac{\nabla \bar{\omega} \cdot \mathbf{J}_\omega}{(a_1 - \bar{\omega})(\bar{\omega} - a_2)} \quad (16)$$

$$\text{and } \frac{dE}{dt} = \int_D d\mathbf{r} \nabla \psi \cdot \mathbf{J}_\omega \quad (17)$$

We note that  $(a_1 - \bar{\omega})(\bar{\omega} - a_2) \geq 0$ . This expression shows that the entropy production is maximal when the current has a direction opposite to the one of the vorticity gradient.

We want to impose an anisotropic constraint on the turbulent current  $\mathbf{J}_\omega$  ; we put :

$$C_1(\mathbf{r}) \frac{(\mathbf{J}_\omega \cdot \mathbf{e}_1(\mathbf{r}))^2}{2} + C_2(\mathbf{r}) \frac{(\mathbf{J}_\omega \cdot \mathbf{e}_2(\mathbf{r}))^2}{2} = 1 \quad (18)$$

where the two vectors  $\mathbf{e}_1$  and  $\mathbf{e}_2$  (depending on  $\mathbf{r}$ ), and the values of  $C_1$  and  $C_2$  will be specified latter. We search for the current  $\mathbf{J}_\omega$  which maximize the entropy production (16), while verifying the energy conservation (17), the anisotropic constraint (18) and the global constraint on  $\mathbf{J}_\omega$  :  $\int_D d\mathbf{r} \mathbf{J}_\omega = 0$ . We thus consider the critical points of the functional :

$$\frac{dS}{dt} - \beta \frac{dE}{dt} - \sum_{i=1,2} \int_D d\mathbf{r} \alpha(\mathbf{r}) C_i(\mathbf{r}) (\mathbf{J}_\omega \cdot \mathbf{e}_i)^2 + (\mathbf{e}_z \wedge \mathbf{V}) \cdot \int_D d\mathbf{r} \mathbf{J}_\omega,$$

where  $\beta$ ,  $\alpha(\mathbf{r})$  and  $-\mathbf{e}_z \wedge \mathbf{V}$  are Lagrange parameters associated to the constraints. The first variations of this functional lead to :

$$\mathbf{J}_\omega = - \sum_{i=1,2} \nu_i \left[ \left( \nabla \bar{\omega} + (a_1 - \omega)(\omega - a_2) \left( \beta \nabla \bar{\psi} - \mathbf{e}_z \wedge \mathbf{V} \right) \right) \cdot \mathbf{e}_i \right] \mathbf{e}_i \quad (19)$$

with  $\nu_i = -1/(\alpha C_i (a_1 - \bar{\omega}) (\bar{\omega} - a_2))$ .

Using the energy constraint (17) and the condition on the zero global average for  $\mathbf{J}_\omega$ , we compute the entropy production :

$$\frac{dS}{dt} = \int_D d\mathbf{r} \sum_{i=1,2} \frac{(\mathbf{J}_\omega \cdot \mathbf{e}_i)^2}{\nu_i (a_1 - \bar{\omega}) (\bar{\omega} - a_2)}$$

Noting that  $(a_1 - \bar{\omega}) (\bar{\omega} - a_2) > 0$ , we conclude that if the diffusivities  $\nu_i$  are strictly positive, the entropy variation is actually an entropy production. With strictly positive diffusivities, we can also conclude, that if the flow converges towards a stationary state, the entropy production must vanish and thus the current  $\mathbf{J}_\omega$  must be zero. In such a case, from (19) we obtain  $\mathbf{e}_z \wedge \mathbf{V} = \nabla \left( \beta (a_1 - a_2) \bar{\psi} + \log(\bar{\omega} - a_2) - \log(a_1 - \bar{\omega}) \right)$ . The constant  $\mathbf{e}_z \wedge \mathbf{V}$  being a gradient must be equal to zero. This equation can then be integrated to. This yields :

$$\bar{\omega} = -\Delta \bar{\psi} = \frac{a_1 + a_2}{2} - \tanh \left( \frac{a_1 - a_2}{2} (\beta \bar{\psi} + \alpha) \right) \quad (20)$$

This is the equations of the statistical equilibrium, which is a stationary state of the Euler equations. We thus conclude, that if the equations for the coarse-grained field, with turbulent current (19), converge; they converge towards a statistical equilibrium. We will call these equation anisotropic relaxation equations.

Let us determine  $\beta$  and  $\mathbf{V}$ . For this let us denote  $\mathbf{A} \equiv \sum_{i=1,2} \int_D d\mathbf{r} \nu_i (a_1 - \bar{\omega}) (\bar{\omega} - a_2) \mathbf{e}_i^T \mathbf{e}_i$ , ( $T$  is the transposition operator).  $\mathbf{A}$  is thus an order two symmetric tensor),  $\mathbf{b} = \sum_{i=1,2} \int_D d\mathbf{r} \nu_i (a_1 - \bar{\omega}) (\bar{\omega} - a_2) \nabla \bar{\psi} \cdot \mathbf{e}_i$  (2d vector) and  $c = \sum_{i=1,2} \int_D d\mathbf{r} \nu_i (a_1 - \bar{\omega}) (\bar{\omega} - a_2) (\nabla \bar{\psi} \cdot \mathbf{e}_i)^2$  (scalar).  $M = \begin{pmatrix} \mathbf{A} & -\mathbf{b} \\ -\mathbf{b} & c \end{pmatrix}$  is a 3X3 symmetric matrix. We then express the energy conservation (17) and the property of the zero average for  $\mathbf{J}_\omega : \int_D d\mathbf{r} \mathbf{J}_\omega = 0$ . This yields three equations to determine the three variables  $\beta$  and  $\mathbf{V}$  :

$$M \begin{pmatrix} \mathbf{e}_z \wedge \mathbf{V} \\ \beta \end{pmatrix} = \begin{pmatrix} \sum_{i=1,2} \int_D d\mathbf{r} \nu_i (\nabla \bar{\omega} \cdot \mathbf{e}_i) \mathbf{e}_i \\ -\sum_{i=1,2} \int_D d\mathbf{r} \nu_i (\nabla \bar{\omega} \cdot \mathbf{e}_i) (\nabla \bar{\psi} \cdot \mathbf{e}_i) \end{pmatrix} \quad (21)$$

We prove in note <sup>1</sup> that, for strictly positive  $\nu_1$  et  $\nu_2$ ,  $M$  is invertible, except for a flow with

<sup>1</sup>Let us prove that the symmetric matrix  $M$  is invertible. For this, let us consider  $M$  as defining a quadratic form, and let us prove that it is definite positive. Using the expressions for  $\mathbf{A}$ ,  $\mathbf{b}$  and  $c$ , the linearity of the integral and the relation :  ${}^t \mathbf{y} \mathbf{e}_i \mathbf{e}_i \mathbf{y} = (\mathbf{e}_i \cdot \mathbf{y})^2$ , a straightforward computation leads to :  $({}^t \mathbf{y} x) M \begin{pmatrix} \mathbf{y} \\ x \end{pmatrix} = \int_D d\mathbf{r} \sum_{i=1,2} \nu_i (a_1 - \omega) (\omega - a_2) (\mathbf{e}_i \cdot (\mathbf{y} - \mathbf{x} \nabla \psi))^2$ . Given that  $(a_1 - \omega) (\omega - a_2) > 0$ , this computation shows that the quadratic form is positive ( $\geq 0$ ). Moreover, noting that  $\mathbf{e}_1$  and  $\mathbf{e}_2$  are orthonormal, we conclude that if  $\nu_1$  and  $\nu_2$  are strictly positives,  $({}^t \mathbf{y} x) M \begin{pmatrix} \mathbf{y} \\ x \end{pmatrix}$  can be zero only if  $(\mathbf{y} - \mathbf{x} \nabla \psi)$  is null on the whole domain. This would imply that  $\nabla \psi$  be constant on the domain. With periodic boundary conditions, this is possible only if  $\psi = 0$ , that is for a flow without motion.

$\psi = 0$ , that is except for an identically zero velocity.

We have obtained relaxation equations, which have the property to increase the entropy while conserving energy. We will now specify the vectors  $\mathbf{e}_i$  and the values of the diffusivity  $\nu_i$ . For this we impose a diffusivity  $l^2\sigma$  in the stable direction of the strain tensor  $\mathbf{e}_\sigma$  and zero in the unstable direction of the strain tensor  $\mathbf{e}_\sigma$ . This choice is the one which allow to best approximate the deterministic approximation of the turbulent current, obtained in section 3.1, while insuring that the diffusivities are positive. We then obtain the following parameterization :

$$\frac{\partial \bar{\omega}}{\partial t} + \bar{\mathbf{u}} \cdot \nabla \bar{\omega} = \nabla \cdot \left( l^2 \sigma [(\nabla \bar{\omega} + \beta (a_1 - \bar{\omega}) (\bar{\omega} - a_2) \nabla \psi) \cdot \mathbf{e}_\sigma] \mathbf{e}_\sigma \right) \quad (22)$$

with

$$\beta = - \frac{\int_D d\mathbf{r} \sigma \nabla \bar{\omega} \cdot \mathbf{e}_\sigma \nabla \bar{\psi} \cdot \mathbf{e}_\sigma}{\int_D d\mathbf{r} \sigma (a_1 - \bar{\omega}) (\bar{\omega} - a_2) \left( \nabla \bar{\psi} \cdot \mathbf{e}_\sigma \right)^2} \quad (23)$$

To obtain this equation for  $\beta$  (23), we have used (21) and neglect the effect of the Lagrange parameter  $\mathbf{V}$  (see 19). We have thus assumed  $\mathbf{V} = 0$ . (in section 5, we will use the relaxation equation to model flow evolutions. we have done computation with  $\mathbf{V} \neq \mathbf{0}$ , using (21), but without noting any important difference with the case  $\mathbf{V} = \mathbf{0}$ )

The main hypothesis of the model (22) is that the local, destabilizing action of the positive part of the strain tensor be replaced by the non local non destabilizing drift term :  $\beta (a_1 - \bar{\omega}) (\bar{\omega} - a_2) \nabla \bar{\psi}$ . This terms insures the energy conservation.

From a numerical point of view, the implementation of this equation has the same level of complexity as the implementation of the Navier-Stokes equation. All what is further needed is the diagonalization of a 2X2 symmetric matrix to determine the strain tensor directions and the mean strain  $\sigma$ . The computation cost of these operations (of order  $N$ , where  $N$  is the number of degrees of freedom) is negligible with respect to the computation of the fast Fourier transform needed to evaluate the nonlinear terms in a pseudo-spectral code (of order  $N \log N$ ).

In next section, we will compare this model with usual parameterizations of two-dimensional and geophysical flow computations. We will show that they give more precise results for the same resolution (or equivalently for the same computational time). This will characterize an important predictability gain for the determination of the flow evolution.

## 5 Comparison of the anisotropic relaxation equations with commonly used models

The aim of this chapter is to determine the efficiency of the anisotropic relaxation equations when compared with other models of small scale turbulence. We consider the

regime of vortex merging and filamentation. We study two types of flows : firstly the merging of four vortices, which leads to a stable dynamics (the position of the final vortex is always on the center of the domain) and secondly the merging of 50 vorticity patches which leads to successive vortex merging and for which the positions of the vortices is very sensitive to the initial parameterization. In order to compare different models, we will use as a reference, high resolution direct numerical computations of the flow.

We will compare the anisotropic relaxation equation with the following parameterizations :

- direct numerical simulations with the Navier Stokes equations (13) (denoted DNS)
- with hyperviscous parameterization, where the Laplacian operator is replaced by a bi-Laplacian :

$$\frac{\partial \omega}{\partial t} + \mathbf{u} \cdot \nabla \omega = \nu \Delta \Delta \omega \quad (24)$$

(denoted HV). Such an hyperviscous parameterization is commonly used in two-dimensional and geophysical flow computation. It is not based on any physical ground. However, the bi-Laplacian has the effect to stabilize the computation whereas it actually acts only on very small scales (higher effective Reynolds number). It usually dissipates few energy. It leads to some unphysical spurious description of the small scale structures, due to the non-respect of the maximum principle of the Navier Stokes equation (the maxima of the vorticity may increase in the hyperviscous case)

- the Smagorinsky model [13] (denoted SMA). The Smagorinsky model uses an isotropic viscosity  $\nabla \cdot (\nu \nabla \omega)$  but with a non-constant viscosity. The viscosity is taken proportional to the mean shear  $\sigma : \nu(\mathbf{r}) = l^2 \sigma(\mathbf{r})$ . This parameterization takes into account of the importance of the strain for the transport to small scales of the flow structures. However the diffusion acts indistinctly in all directions (isotropic). This model is commonly used in geophysical fluid computation.

Concerning the anisotropic relaxation equation, we will alternatively use either the equations (22) and (23) (denoted RELANI) or the equations (22) with a local computation of the Lagrange parameter  $\beta$  for the energy conservation (denoted RELANILOC). In this last case we will determine  $\beta$  with (22), but with an evaluation of the integrals in subdomains  $D_i$  large compared to the resolution scale  $l$ , but smaller than the domain scale. For instance, for low resolution computation with 256X256 degrees of freedom, we will evaluate  $\beta$  in 12X12 subdomains. We will also consider the isotropic relaxation equations (Robert and Sommeria [12]) (denoted REL)

For all of these models, the diffusivities  $\nu$ , or the parameters  $l$ , are always chosen as small as possible for the numerical computation to be stable.

We quantify the error of the low resolution computation, with respect to reference high-resolution computation (field denoted by the subscript  $_{ref}$ ), by evaluating the velocity relative error :  $E_r \equiv \int_D d\mathbf{r} (\mathbf{u} - \mathbf{u}_{ref})^2 / \int_D d\mathbf{r} \mathbf{u}_{ref}^2$  or the vorticity relative error :  $E_{r-\omega} \equiv \int_D d\mathbf{r} (\omega - \omega_{ref})^2 / \int_D d\mathbf{r} \omega_{ref}^2$ . (these quantities are evaluated in the Fourier space,

using a number of components corresponding to the low resolution fields).

We first consider an initial condition made of four vortices (Fig. 4). Initially four vorticity patches with vorticity  $a_1 = 2.942$  are in an ambient vorticity  $a_2 = -0.263$ . The edges of the vortex patches are smoothed to avoid numerical problems for initial times. The position of each vortex is slightly moved, in order to break the apparent symmetry of the initial condition. We will use as reference computation a Navier-Stokes simulation with resolution 1024x1024 (DNS.Euler4.1024). Numerical parameters are given in table 4. The corresponding Reynolds number, based on the domain scale, is then 400 000. Fig. 4 shows the vorticity field evolution. This typical experiment of vortex merging show the filamentation followed by a very slow organization towards a stationary state. The energy loss between times  $T = 0$  and  $T = 100$  is 0.7%. We thus consider this computation as close to the inertial limit.

Fig. 5 shows the evolution of the velocity relative error for 4 computations with resolutions 256X256 and with respective parameterizations : Navier Stokes (DNS.Euler4.256), isotropic relaxation equation (constant diffusivities) (REL.Euler4.256), anisotropic relaxation equations (RELANI.Euler4.256) and anisotropic relaxation with local conservation of the energy (RELANILOC.Euler4.256). Table 4 gives the numerical parameters for each of these computations. Fig. 5 shows that the maximal relative error is 5%. In this case, the numerical evolution is thus easily predictable. After a quasi-exponential growth, the error saturates and oscillates together with the position the oscillation of the slightly asymmetric vortex. The oscillations reflect the oscillation with respect to the one of the vortex in the reference computation. The anisotropic relaxation equation with local conservation of the energy give clearly the best results.

Fig. 6 compares the evolution of the vorticity relative error for the anisotropic relaxation equations with local energy conservation (RELANILOC.Euler4.256), hyperviscosity (HV.Euler4.256), and the Smagorinsky model (SMA.Euler4.256). For short times, the anisotropic relaxations give a slightly better result than the hyperviscous computation. However for larger times, the two model are not better one than the other. Both models are however much more efficient than the Smagorinsky model. In [14], we present a more complete study and show that same conclusions are obtained for the study of the evolution of the velocity relative error. For a smaller resolution 128X128, the anisotropic relaxation equations turn out to give better results than the hyperviscous parameterization.

The previous computation is a typical merging of a small number of vortices. The initial configuration of these vortices leads to a rapid stabilization of a single structure. In order to study the effect of the parameterizations for a more complex dynamical evolution, we will consider an initial vorticity field composed by 50 vorticity patches, with random initial positions. We make the same study as in the previous case, comparing the efficiency of the different parameterizations in a low resolution computation (256X256), using as a reference a larger resolution computation (1024X1024). As in the previous case, the Navier-

Stokes or Smagorinsky parameterizations lead to a much less efficient computation than the hyperviscous or anisotropic relaxation equations ones. For instance, Fig. 7, for time  $T = 45$ , clearly shows that the Navier-Stokes equation do not even reproduce the qualitative properties of the vorticity fields for large time. This is due to the spurious effect of the viscous dissipation. The Smagorinsky model also leads to a too important diffusion. (As in previous computations, we always use the smaller viscosity or parameter  $l$ , compatible with the stability of the computation. Numerical parameters are reproduced on table 4.)

Fig. 8 shows the evolution of the velocity relative error for three low resolution (256X256) computations : hyperviscous (HV.Euler50.256), anisotropic relaxation (RELANI.Euler50.256) and anisotropic relaxation with local energy conservation (RELANILOC.Euler50.256). We use as a reference an hyperviscous computation with resolution 1024X1024. For smaller times, the three computations give equivalent results : a quasi-exponential evolution of the error, probably associated to the intrinsic instability of the initial condition. However, after a stage of several vortex merging, the anisotropic relaxation equations give much better results than the hyperviscous ones. This is illustrated by Figs 8 and 7. This last figure show that the position and the structures of the two final vortices is better reproduced. We propose the following interpretation : whereas the vortex motion is very sensitive to the initial condition, the result of the vortex merging depends less on the detail initial condition. It rather depends on the dynamical invariants (the global vorticity, the energy). The relaxation equation which explicitly conserve the energy, and which describes the vorticity mixing in accordance with the statistical properties of the system lead to better results than the hyperviscous or the other parameterization studied here. We thus observe a *statistical saturation* of the error during this stage.

These results show that the Navier-Stokes equation is very clearly the poorer model of two dimensional decaying turbulence. To compute the error, we have used, as a reference, an hyperviscous type computation. In order for the results to be non ambiguous, we have shown in [14] that all the conclusions we give here are also valid when a comparison is made with Navier-Stokes high resolution computations (HV.Euler50.1024) (see also figure 7).

We conclude that in any situations, hyperviscous parameterizations and anisotropic relaxation equations lead to much better results than Navier-Stokes equation or the Smagorinsky model. The difference between hyperviscous and anisotropic relaxation equations computations is less important. However for small resolution (HV.Euler4.128) or for very complex flow evolution, the anisotropic relaxation equations give better results than the hyperviscous parameterization.

Our validation by comparison with higher resolution computation, does not allow us to compare different models for very large times. However, we think that the relaxation equation will then give much better results than the hyperviscous ones, because they exactly conserve the energy, because they treat vorticity mixing as far as possible according to the physical processes responsible for this mixing, and because they converge towards equilibrium states of the Euler equation. On the contrary hyperviscous model are not based



on any physical ground.

We conclude by stating that similar results have been obtained in the context of the Quasi-Geostrophic dynamics (not reported, see [14]). Due to the slowing down of the dynamical mixing of the potential vorticity for small Rossby deformation radius  $R$  (the interaction is screened at a typical scale  $R$ ), the relative efficiency of the anisotropic relaxation equations is even more evident in such a case.

## 6 Discussion

For geophysical flows, the scale at which the microscopic diffusion is relevant is so small that any numerical model of oceans or atmosphere implicitly assumes a small scale parameterization. In such physical situations, lots of phenomenon occur at the unresolved scales : convection, interaction with boundary, three dimensional turbulence at smaller scales, leading to molecular diffusion, etc ... For this reason, the fundamental equation to start with to describe such flows is not even clear [1]. It is however generally recognized that the dynamics of geophysical flows is two-dimensional like (inverse energy cascade) and that the dynamics of the potential vorticity plays a major role. In order to parameterize the potential vorticity mixing, we have considered the simplest model having the main properties of large scale geophysical flows : the barotropic Quasi-geostrophic model. As the equations are formally equivalent, we have led our study mainly in the 2D incompressible Euler-equation framework. All the results obtained are valid for both of these models, and may be straightforwardly generalized to the multi-layered Quasi-Geostrophic model. The problem we have addressed is to describe the evolution of the coarse-grained vorticity, the fundamental equation being the Euler (or QG) equations. In this study, we have considered a regime of freely decaying turbulence, with vortex merging and filamentation. As we mainly study this transient behavior, this study also apply for the two-dimensional Navier-Stokes equations (or viscous QG) with a molecular viscosity acting on a scale much smaller than the resolved one.

In section 2, we have first defined the coarse-graining. We have then shown that the parameterization problem is equivalent to the determination of a turbulent current. We have obtained at leading order a deterministic approximation of the turbulent current : the action of the strain tensor on the gradient of the vorticity[16, 15, 14]. We have shown using numerically obtained vorticity fields that this approximation is a good one in the regime of vortex merging and filamentation. The leading contribution comes from the part of the turbulent current which is absent in the case of an ensemble average (like in usual Reynolds tensor). This shows that the turbulent current is dominated by systematic correlation between resolved and unresolved scale. This essentially deterministic process is qualitatively associated to structures (filaments) passing from resolved to unresolved scales). This deterministic approximation exactly conserves the energy.

This deterministic approximation acts on the vorticity field as a positive viscosity in

the stretching direction of the strain tensor, and as a negative viscosity in the expansion direction. Due to this last contribution, a numerical model using directly this approximation would lead to numerical instabilities. In order to obtain stable equations, respecting the actual diffusion in the contraction direction, and the energy conservation, we look for equations maximizing the mixing entropy for the vorticity, while imposing these dynamical constraints. We obtain *anisotropic relaxations equations* which have the further property to relax towards the statistical equilibrium of the Euler-equation.

Some entropy based parameterization of the turbulent current have been proposed previously in the case of topography dominated flows, by Holloway (see [22] for a review or [23] for some application in the context of oceanographic flows). The maximum entropy production principle has been proposed in [12], but an isotropic turbulent current was then imposed. The maximum entropy production principle has no theoretical or physical ground. The anisotropic relaxation equations do not for instance describe correctly what happens in the strain tensor stretching direction. We use here this principle as a trick to obtain stable equations, with given constraints, and respecting the statistical tendency of the vorticity mixing.

In order to show the interest of the anisotropic relaxation equations, we have compared its efficiency with the Navier-Stokes equations, or other usual parameterizations such as the Smagorinsky model or the hyperviscous model. We have compared the results with higher resolution Navier-Stokes or hyperviscous computations. As they overestimate strongly the diffusion, the Navier-Stokes or the Smagorinsky model give clearly the worst results. The anisotropic relaxation equations give better results than the hyperviscous model, for complex flow evolution, for smaller resolutions, or for the Quasi-Geostrophic model.

The results we have obtained clearly show that the anisotropic relaxation equations allows an increase of the predictability with respect to other parameterizations. We note however that we have suppose a complete knowledge of the initial condition. The real problem of predictability for geophysical flows is much more complex, as lots of error sources have to be taken into account. We have studied only the effect of the parameterization of the potential vorticity mixing.

Let us conclude on a discussion on the limitations of this work and on its possible interest in a wider context. We have First we have studied the regime of vortex merging and strong filamentation. However, for inviscid two-dimensional freely decaying turbulence, on the latter stage of the evolution of the flow, the coarse-grained field is close to a stationary state. In this different regime, no more structures are transported from larger to smaller scales (scale separation). In such a case, the main contribution to the turbulent current probably comes from the stochastic part of the current. The effect of these fluctuations is a very slow modification of the structure of the quasi-stationary coarse-grained flow. An ensemble average is probably the best way to address such a relaxation. We note the application of a quasi-linear theory in [11] which may be of interest for this regime.

In the situation we have studied, because the processes are very rapid, the effect of

a very small viscosity (acting on scales much smaller than the resolution one) is actually negligible. However, in the stage of a quasi-stationary state relaxation, the effect of a very small viscosity would probably be very important, as it should determine the distribution of the unresolved scale vorticity. A statistical mechanics based approach is proposed in [26]. There a crude closure, using the simplest energy-entropy statistical theory for flow with topography, is proposed. In [25] the effect of a small forcing and dissipation is also considered.

Another improvement of our work may be done by the description, not only of the averaged but also of the higher vorticity moments. In [24] an equation hierarchy is derived, to describe these moment evolution. This hierarchy is then closed using a maximum entropy production principle. Such ideas have been applied in the context of a barotropic ocean model [25].

The current computational power allows to make very high resolution simulations of the two-dimensional Navier Stokes equations. In such a case, the precise simulation of rapid physical phenomena does not necessitate any parameterization. However, for more complex physical situations, for very long time simulations or for more complex geophysical flow models, the necessity to use good small scales parameterizations is evident. Let us give some examples. In the modeling of Jupiter's troposphere, we have shown that the very small value of the Rossby deformation radius renders the potential vorticity dynamics very slow [27]. The very long time then needed, for the flow to organize, does not allow to obtain the characteristic very strong jets typical of Jupiter's vortices, when using Navier-Stokes equations. On the contrary, using relaxation equations permits to model these features very precisely, even using quite low resolution models [27]. For ocean modeling, let us discuss the example of the Zapiola anticyclone, in the Argentina basin, in South Atlantic. In the late 90's, Topeix-Poseidon data has clearly revealed this very strong anticyclonic structure, whereas up to date South Atlantic modeling were not able to reproduce it, or were reproducing a structure much weaker than the observed ones [28]. In [28], for instance, the anticyclone modeling is convincing, using the up to date model resolution. Moreover, for global ocean models, or/and when much longer computational times are needed, for instance for climate modeling, the correct description of such structures would necessitate unavailable computational power. Moreover, as shown by Fig. 7 of this study, for very long time scales, the use of rough parameterization alters the fluctuations of vorticity, or potential vorticity.

The modeling of geophysical flows actually require the best possible parameterization. The analysis we have done could be straightforwardly generalized to the case of multi-layered Quasi-geostrophic models. For z-coordinates models, or isopicnal models in use in geophysical flow modeling, the generalization of the ideas developed in this article should be considered ; the problem being much more simple in models clearly identifying the potential vorticity as a key dynamical variable. We conclude by saying that the modeling of the potential vorticity mixing in geophysical fluid dynamics is only one part of the parameterization

problem, but probably one of the more essential one.

## Acknowledgements

This work has been done during my PHD thesis [14], supervised by R. Robert and J. Sommeria. I thank M.L. Chabanol, P.H. Chavanis and B. Dubrulle for useful comments on this work. It has been partly supported by a *Bourse Lavoisier* of the French *Ministère des Affaires Etrangères* and by the contract COFIN00 *Chaos and Localization in Classical and Quantum mechanics*.

## References

- [1] J. Pedlosky, *Geophysical Fluid Dynamics*, Second Edition. Springer Verlag (1987)
- [2] Z.A. Prandtl, "Bericht über Untersuchungen zur ausgebildeten Turbulenz", *Zs Angew. Math. Mech.* **5** 136-169 (1925)
- [3] D.C. Leslie *Developments in the theory of turbulence*, Clarendon Press, Oxford (1973)
- [4] S.A. Orszag, "Lectures on the statistical theory of turbulence", pp 235-374 in Balian, R. and Peube, J.L., ed., *Fluid Dynamics, New York: Gordon & Breach.* (1977)
- [5] M. Lesieur, *Turbulence in Fluids*. 2d ed . Boston:Kluwer (1990)
- [6] B.E. Launder and D.B. Spalding, *Mathematical models of turbulence*. Academic Press (1972)
- [7] R.H. Kraichnan, "The structure of isotropic turbulence at very high Reynolds number", *J. Fluid. Mech.*, **181** 141-162 (1959)
- [8] C. Basdevant and R. Sadourny, "Modélisation des échelles virtuelles dans la simulation numérique des écoulements bidimensionnels", *J. de Mécanique Th. et App.*, **Numéro spécial** 243-269 (1963)
- [9] R. Robert and J. Sommeria, "Statistical equilibrium states for two-dimensional flows", *J. Fluid. Mech.* **229**, 291-310 (1991)
- [10] J. Miller, "Statistical mechanics of Euler's equation in two dimensions" *Phys. Rev. Lett.* **65** (17), 2137 (1990)
- [11] P.H. Chavanis, "Quasilinear theory of the 2D Euler equation" *Phys. Rev. Lett.* **84**, 5512-5515 (2000)

- [12] R. Robert and J. Sommeria, “Relaxation towards a statistical equilibrium state in two-dimensional perfect fluid dynamics”, *Phys. Rev. Lett.* **69**, 2776-2779 (1992)
- [13] J. Smagorinsky, “General circulation experiments with the primitive equations”. *Mon. Weath. Rev* **91** 3 99-164 (1963)
- [14] F. Bouchet, *Mécanique statistique pour des écoulements géophysiques*. PHD Thesis. Université Joseph Fourier - Grenoble (2001).
- [15] T. Dubos, “Cascade bidimensionnelle d’un traceur: diagnostic dans l’espace physique et modélisation.” Thèse de doctorat de l’université Paris 6 (2001)
- [16] T. Dubos, “Un opérateur de diffusion spatialement sélectif pour le transport d’un traceur passif ou actif par des écoulements de grande échelle” *C. R. Acad. Sci. Paris* **329**, série II, 509-516 (2001)
- [17] J.P. Laval, B. Dubrulle and S. Nazarenko, “Nonlocality of interaction of scales in the dynamics of 2D incompressible fluids” *Phys. Rev. Lett.* **83** 20 4061-4064 (1999)
- [18] J.P. Laval, B. Dubrulle and S. Nazarenko, “Dynamical modeling of sub-grid scales in 2D turbulence” *Physica D: Nonlinear Phenomena*, **142**, 3-4, 231-253 (2000).
- [19] J.P. Laval, B. Dubrulle and S. Nazarenko, “Nonlocality and intermittency in three-dimensional turbulence” *Phys. Fluids* **13** 7 1995-2012 (2000)
- [20] J. Michel and R. Robert, “Large Deviations for Young measures and statistical mechanics of infinite dimensional dynamical systems with conservation law” *Commun. Math. Phys.* **159**, 195-215 (1994)
- [21] R. Robert, “On the statistical mechanics of 2D Euler and 3D Vlasov Poisson equations”, *Comm. Math. Phys.* **212**, 245-256 (2000).
- [22] G. Holloway, “Moments of probable seas: statistical dynamics of Planet Ocean” *Physica D* **133** 199-214 (1999)
- [23] A. Alvarez, J. Tintore, G. Holloway, M. Eby and J.M. Beckers, *J. Geophys. Res.* **99** 16053-16064 (1994)
- [24] R. Robert and C. Rosier, “The modeling of small scales in 2D turbulent flows: a statistical mechanics approach” *J. Stat. Phys.* **86**, 481-515 ( 1997)
- [25] E. Kazantsev, J. Sommeria and J. Verron, “Subgridscale Eddy Parameterization by Statistical Mechanics in a Barotropic Ocean Model” *J.Phys.Ocean.* **28** (6) 1017-1042. (1998)

- [26] M.J. Grote and A. J. Majda, "Crude closure for flow with topography through large-scale statistical theory" *Nonlinearity*, **13**, 3, 569-600 (2000)
- [27] F. Bouchet and T. Dumont, "Emergence of the Great Red Spot of Jupiter from random initial conditions" Submitted à *Journal of Atmospheric Science* (2003)
- [28] A. De Miranda, B. Barnier and W.K. Dewar, "On the dynamics of the Zapiola anticyclone." *J. Geophys.Res.*, **104**, 21,137-21,149, (1999).

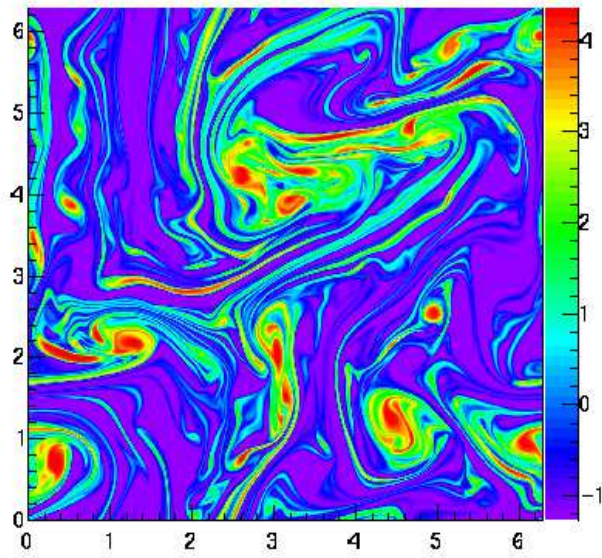
	$\ \cdot\ _2$	$\ \cdot\ _\infty$	$\ \bar{\omega}\ _1 / \ \cdot\ _1$
$\nabla \cdot \mathbf{J}_\omega$	1.14	1.39	7.63
$\nabla \cdot (\bar{\omega} \bar{\mathbf{u}} - \bar{\omega} \bar{\mathbf{u}})$	5.34	7.16	1.64
$\nabla \cdot (\bar{\omega} \bar{\mathbf{u}})$	5.38	7.20	1.64
$\nabla \cdot (\bar{\omega} \bar{\mathbf{u}})$	0.04	0.06	229
$\nabla \cdot (\bar{\omega} \bar{\mathbf{u}})$	0.12	0.19	76.4
$\nabla \cdot \mathbf{J}_d$	1.12	1.35	7.81
$\nabla \cdot \mathbf{J}_s$	0.08	0.14	111

TAB. 1 – Comparison of the contribution of the divergence of the components of the turbulent current, evaluated with several norms  $\|f\|_2 = \sqrt{1/|D| \int_D d\mathbf{r} f^2}$ ,  $\|\cdot\|_\infty = \text{Sup}_D \{|f|\}$ ,  $\|f\|_1 = 1/|D| \int_D d\mathbf{r} |f|$ . The divergence of the turbulent current  $\nabla \cdot \mathbf{J}_\omega = \nabla \cdot \mathbf{J}_d + \nabla \cdot \mathbf{J}_s$  is dominated by the contribution of its deterministic part  $\nabla \cdot \mathbf{J}_d$ . The stochastic part  $\nabla \cdot \mathbf{J}_s = \nabla \cdot (\bar{\omega} \bar{\mathbf{u}}) + \nabla \cdot (\bar{\omega} \bar{\mathbf{u}})$  is dominated by  $\nabla \cdot (\bar{\omega} \bar{\mathbf{u}})$ . This last term would be the only contribution in the case of an ensemble average.

	$\ \cdot\ _2$	$\ \cdot\ _\infty$	$\ \bar{\omega}\ _1 / \ \cdot\ _1$
$\nabla \cdot \mathbf{J}_d$	1.12	1.35	7.81
$\nabla \cdot (\mathbf{J}_d - l^2 \Sigma_{sym} \nabla \bar{\omega})$ (ordre 1)	0.13	0.18	69.0
$\nabla \cdot (\mathbf{J}_d - l^2 \Sigma \nabla \bar{\omega} - \text{ordre 2})$	0.05	0.10	163
$\nabla \cdot (l^2 \Sigma_{sym}^< \nabla \bar{\omega})$	1.36	1.91	6.61
$\nabla \cdot (l^2 \Sigma_{sym}^> \nabla \bar{\omega})$	0.86	1.13	10.8
$\nabla \cdot (\mathbf{J}_d - l^2 \Sigma_{sym}^< \nabla \bar{\omega})$	0.87	1.13	10.8

TAB. 2 – Norm of the difference between the divergence of the deterministic part of the turbulent current  $\nabla \cdot \mathbf{J}_d$  and its first and second order approximations. The leading order approximation of  $\nabla \cdot \mathbf{J}_d$  is correct up to an error of order 10%, for the three norms considered. This error is of the same order as the one corresponding to the stochastic part  $\nabla \cdot \mathbf{J}_s$ .

T = 14.00



T = 14.00

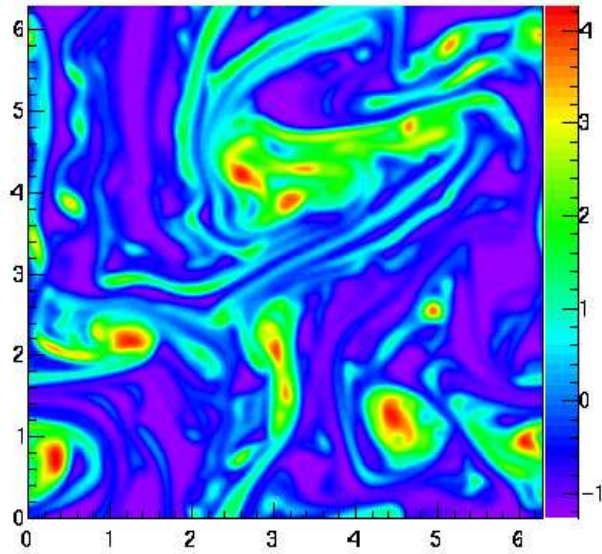


FIG. 1 – Upper picture : a typical vorticity field  $\omega$  for freely decaying turbulence in the regime of filamentation and vortex coalescence (resolution 1024X1024). Lower picture : the corresponding averaged vorticity field  $\bar{\omega}$ , for a Gaussian homogenization at the scale  $l = 2\pi/128 \simeq 0.049$ . Fig. 2 shows the corresponding turbulent current.



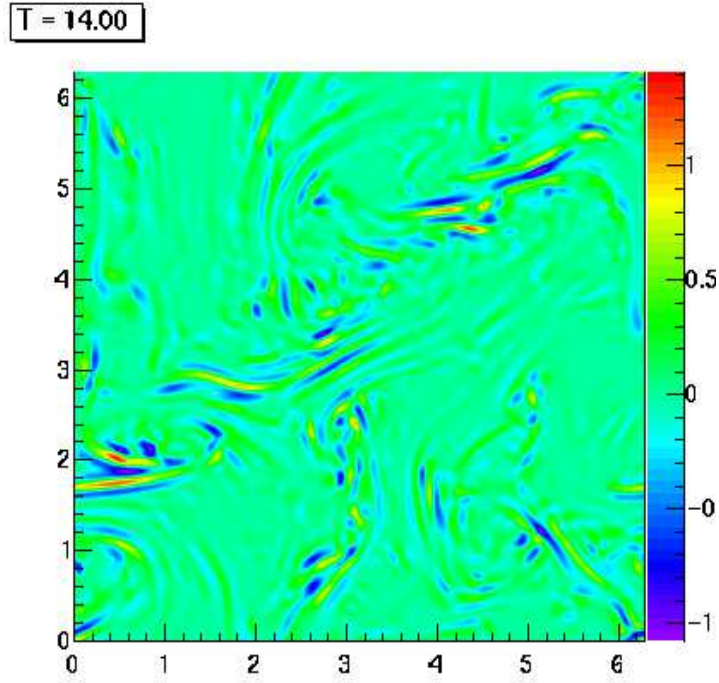


FIG. 2 – The divergence of the turbulent current  $\nabla \cdot \mathbf{J}_\omega$ , computed for a Gaussian homogenization at a scale  $l = 2\pi/128 \simeq 0.049$ , for the vorticity field shown on Fig. 1. The comparison with Fig. 1 illustrates that important values of the divergence of the turbulent current are associated with structures with typical scale  $l$ , especially filaments. Not all structures at scale  $l$  give a strong contribution, but only the ones correlated with a strong mean strain (see Fig. 3).

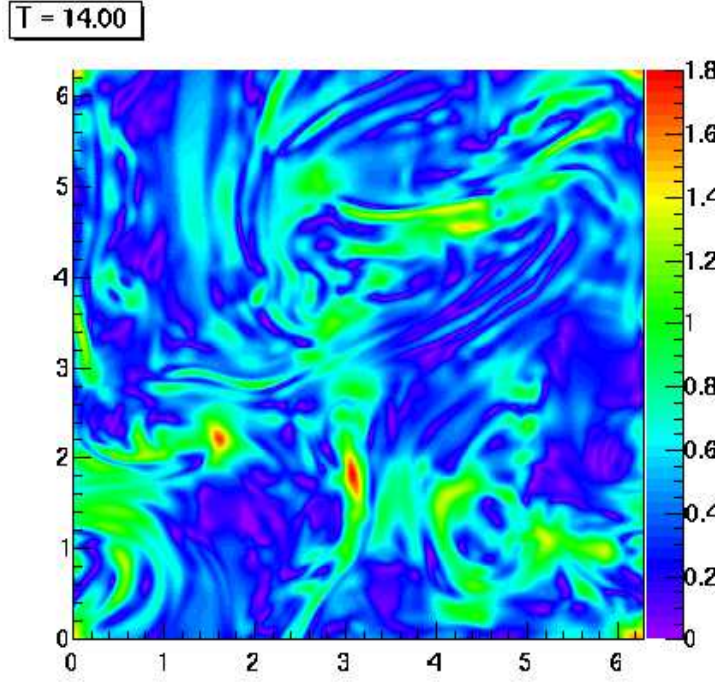


FIG. 3 – The mean strain  $\sigma$  (positive eigenvalue of the symmetric part of the strain tensor) for the velocity field corresponding to the homogenized vorticity  $\bar{\omega}$  (Fig. 1). We note the correlation between areas of strong strain, areas with strong vorticity gradients (Fig. 1) and areas where the divergence of the turbulent current is high (Fig. 2).

Calcul	Résolution	$\nu$ ou $l$	$dt$	$Re$
DNS.Euler4.1024	1024x1024	$1.57 \cdot 10^{-5}$	$6.14 \cdot 10^{-4}$	400 000
REL.Euler4.256	256x256	$6.28 \cdot 10^{-4}$	$2.45 \cdot 10^{-3}$	10 000
RELVAR.Euler4.256	256x256	$1.26 \cdot 10^{-4}$	$2.45 \cdot 10^{-3}$	-
RELANI.Euler4.256	256x256	$1.33 \cdot 10^{-2}$	$2.45 \cdot 10^{-3}$	-
RELANILOC.Euler4.256	256x256	$1.33 \cdot 10^{-2}$	$2.45 \cdot 10^{-3}$	-
DNS.Euler4.256	256x256	$6.28 \cdot 10^{-4}$	$2.45 \cdot 10^{-3}$	10 000
SMA.Euler4.256	256x256	$1.33 \cdot 10^{-2}$	$2.45 \cdot 10^{-3}$	—
HV.Euler4.256	256x256	$1.92 \cdot 10^{-8}$	$2.45 \cdot 10^{-3}$	—
RELANI.Euler4.128	128x128	$2.45 \cdot 10^{-2}$	$4.91 \cdot 10^{-3}$	-
HV.Euler4.128	128x128	$1.53 \cdot 10^{-7}$	$4.91 \cdot 10^{-3}$	—

TAB. 3 – Numerical parameters for the computations of the coalescence of four vortices

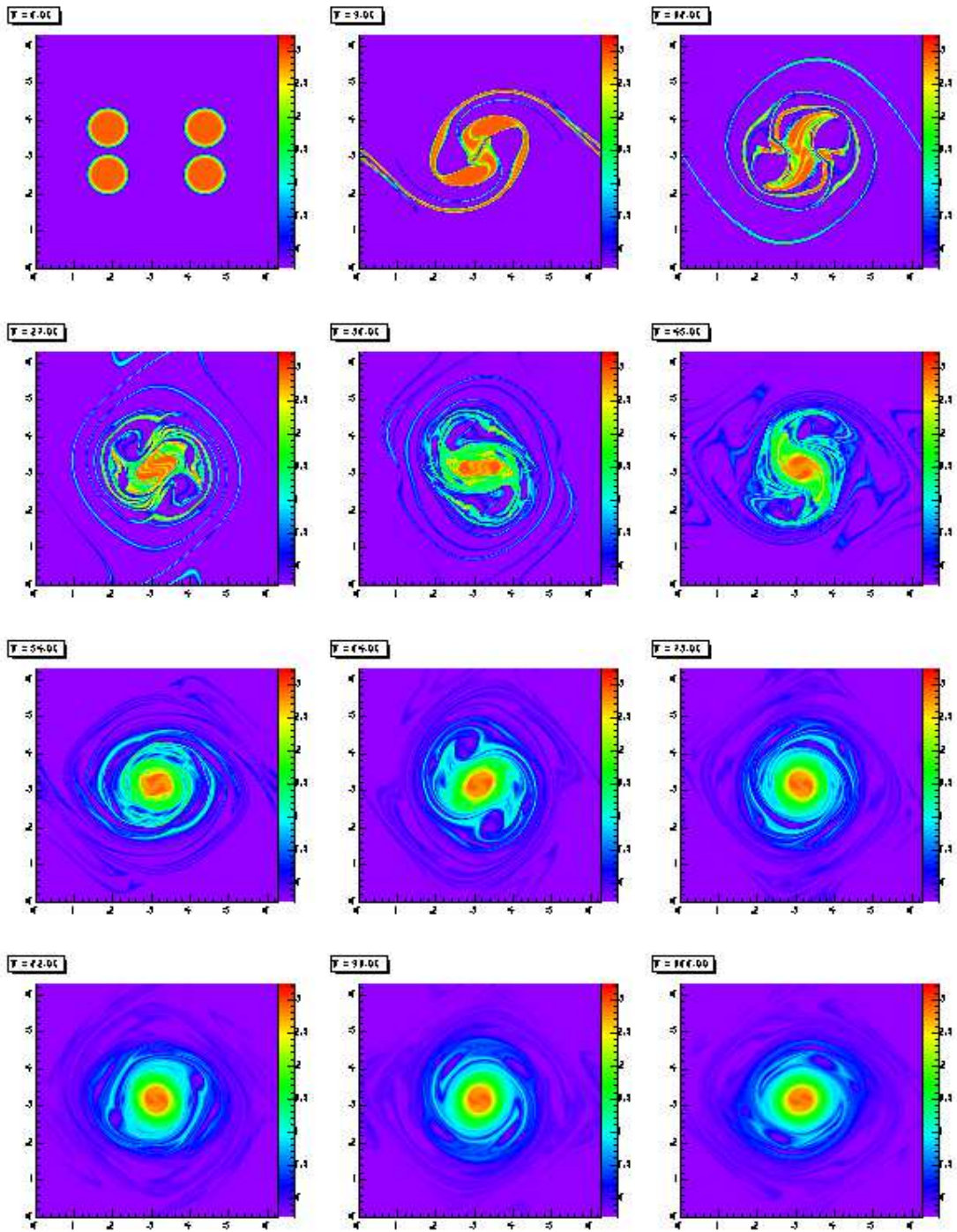


FIG. 4 – Vorticity evolution for the coalescence of four vortices. This computation uses a Navier-Stokes model, with resolution  $1024 \times 1024$  (DNS.Euler4.1024). Time goes from  $T = 0$  to  $T = 99$ . We consider this computation as representative of the inertial limit (energy loss of 0.7% between  $T = 0$  and  $T = 100$ ).

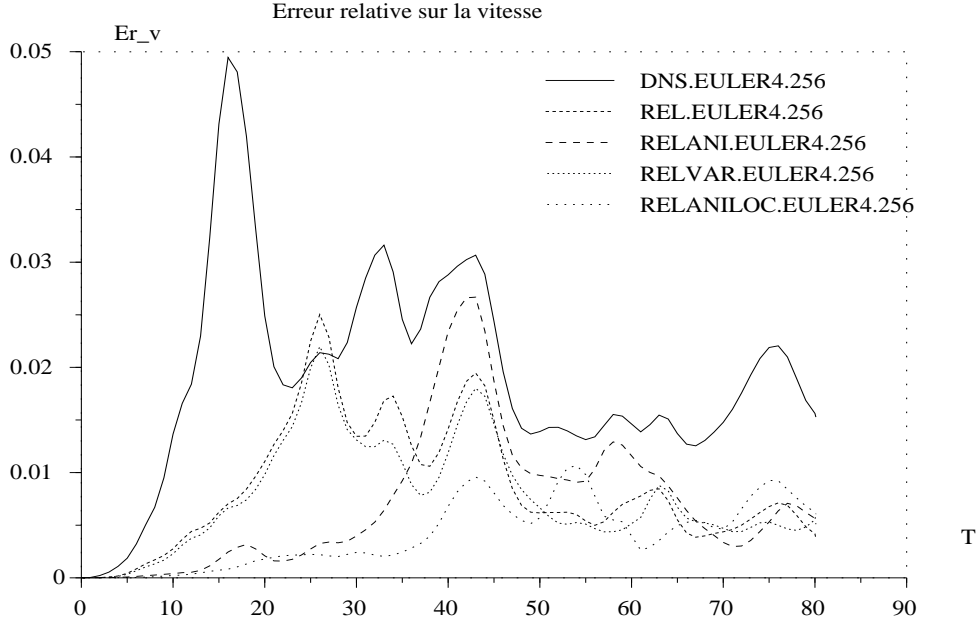


FIG. 5 – Velocity relative error on the low resolution computation, for the coalescence of four vortices, for parameterizations of small scales with respectively : a constant diffusivity (Navier-Stokes) (DNS.Euler4.256), isotropic relaxation equations with constant diffusion (REL.Euler4.256), anisotropic relaxation equations (RELANI.Euler4.256) and anisotropic relaxation equations with local energy conservation (RELANILOC.Euler4.256).

Calcul	Résolution	$\nu$ ou $l$	$dt$	$Re$
DNS.Euler50.1024	1024x1024	$3.14 \cdot 10^{-5}$	$6.14 \cdot 10^{-4}$	200 000
DNS.Euler50.1024	1024x1024	$5.99 \cdot 10^{-11}$	$6.14 \cdot 10^{-4}$	-
RELANI.Euler50.256	256x256	$1.33 \cdot 10^{-2}$	$2.45 \cdot 10^{-3}$	-
RELANILOC.Euler50.256	256x256	$1.33 \cdot 10^{-2}$	$2.45 \cdot 10^{-3}$	-
HV.Euler50.256	256x256	$1.92 \cdot 10^{-8}$	$2.45 \cdot 10^{-3}$	—

TAB. 4 – Numerical parameters for the various parameterization of the coalescence of 50 vorticity patches.

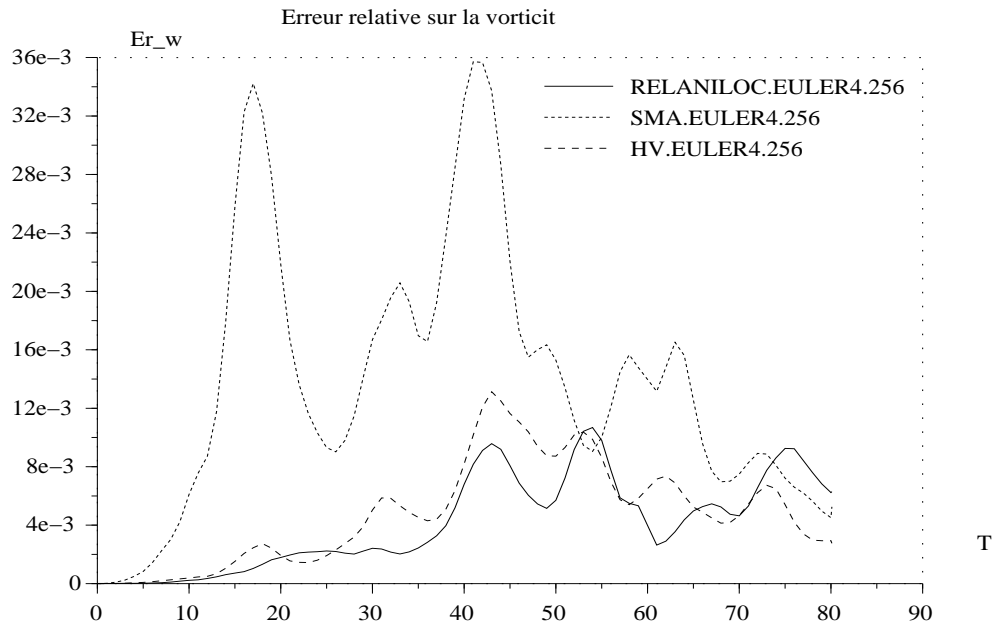


FIG. 6 – Same as Fig. 5, but for the Smagorinsky model (SMA.Euler4.256), the anisotropic relaxation equation (RELANI.Euler4.256) and an hyperviscous parameterization (HV.Euler.4.256); for computations with resolution 256x256.



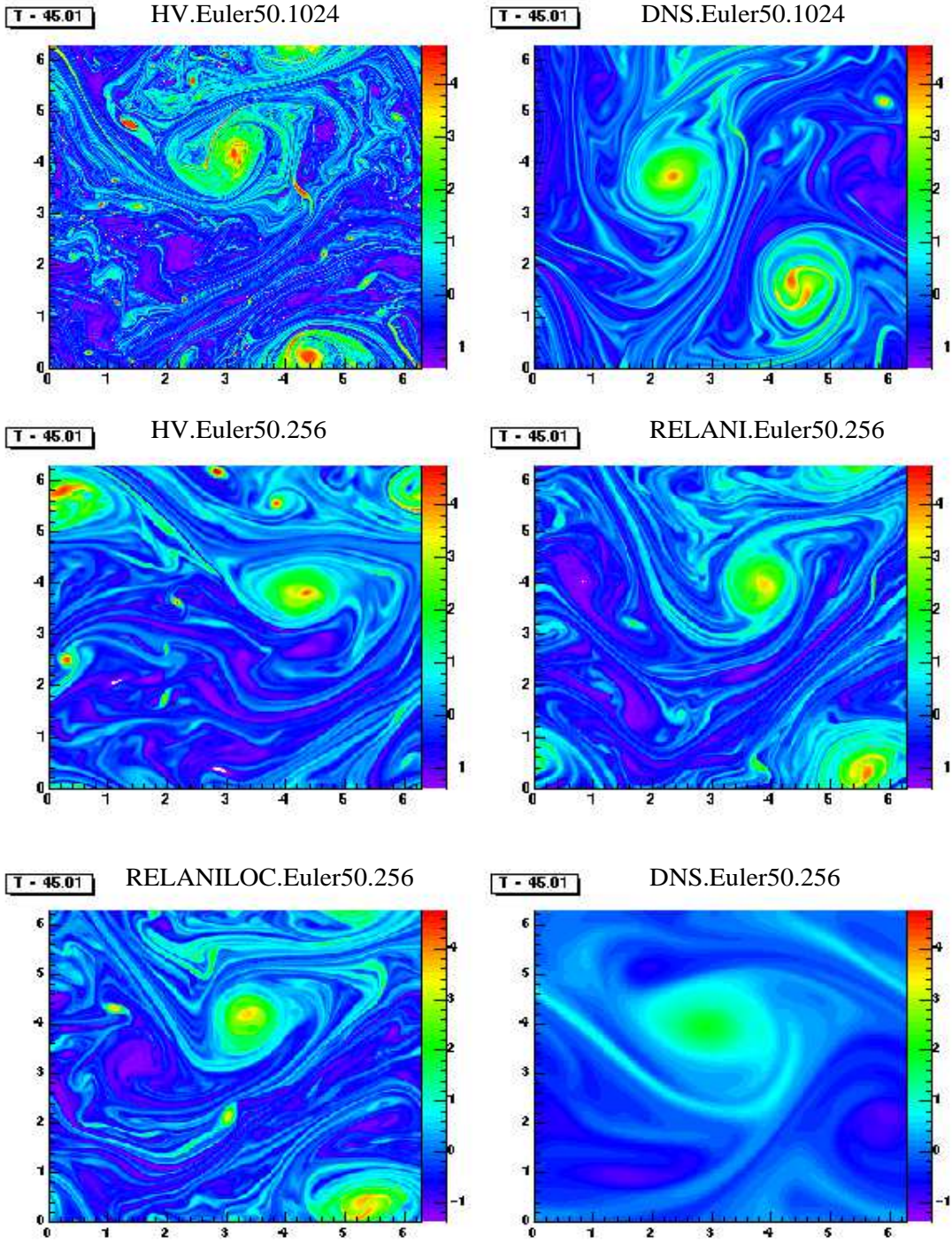


FIG. 7 – Comparison of vorticity field, obtained at time  $T = 45.01$ , from the same initial condition, for two different high resolution computations : hyperviscous (HV.Euler50.1024) and Navier Stokes (DNS.Euler50.1024) ; and four low resolution computations with different small scale turbulence parameterization : hyperviscosity (HV.Euler50.256), anisotropic relaxation equations (RELANI.Euler50.256), anisotropic relaxation equations with local energy conservation (RELANILOC.Euler50.256) and Navier Stokes (DNS.Euler50.256).

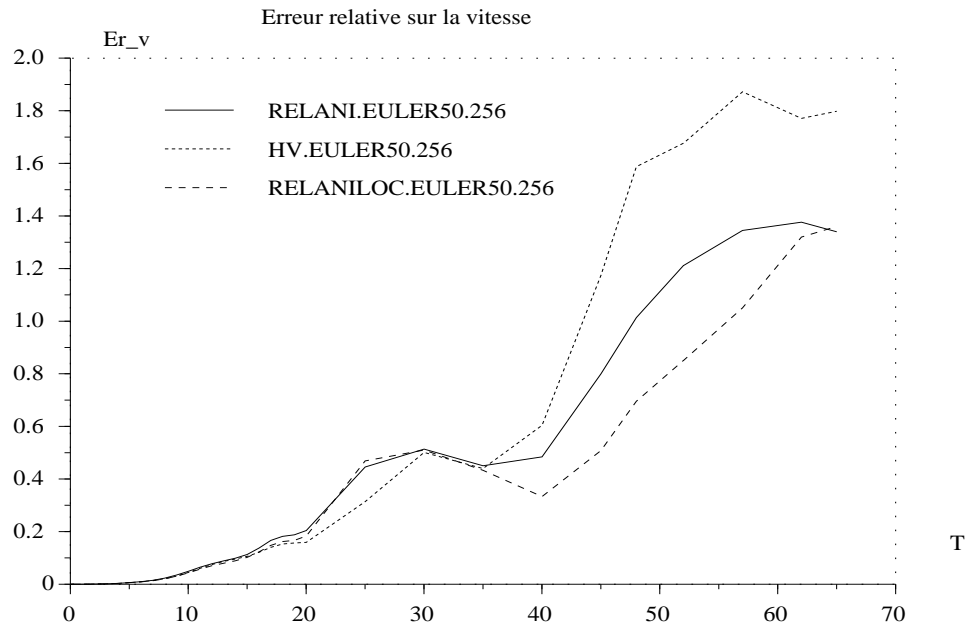


FIG. 8 – Velocity relative error versus time, for three low resolution computations (256x256), with different small scale turbulence parameterization : anisotropic relaxation equations (RELANI.Euler50.256), hyperviscous model (HV.Euler50.256) and anisotropic relaxation equations with local energy conservation (RELANILOC.Euler50.256). The initial condition is made of 50 vorticity patches with random positions. The reference computation is a 1024X1024 resolution hyperviscous one (HV.EULER50.1024)